

Lightning declines over shipping lanes following regulation of fuel sulfur emissions

Chris J Wright^a, Joel A Thornton^a, Lyatt Jaeglé^a, Yang Cao^b, Yannian Zhu^b, Jihu Liu^b, Randall Jones II^a, Robert H Holzworth^c, Daniel Rosenfeld^d, Robert Wood^a, Peter Blossey^a, and Daehyun Kim^{a,e}

^aUniversity of Washington, Department of Atmospheric Sciences, Seattle, WA, 98195

^bNanjing University, School of Atmospheric Sciences, Nanjing, China, 210023

^cUniversity of Washington, Department of Earth and Space Sciences, Seattle, WA, 98195

^dThe Hebrew University of Jerusalem, Institute of Earth Sciences, Jerusalem, Israel, 91904

^eSeoul National University, Department of Atmospheric Science, Seoul, South Korea, 08820

Correspondence: Joel A Thornton (joelt@uw.edu)

Abstract. Aerosol interactions with clouds represent a significant uncertainty in our understanding of the Earth system. Deep convective clouds may respond to aerosol perturbations in several ways that have proven difficult to elucidate with observations. Here, we leverage the two busiest maritime shipping lanes in the world, which emit aerosol particles and their precursors into an otherwise relatively clean tropical marine boundary layer, to make headway on the influence of aerosol on deep convective clouds. The recent seven-fold change in allowable fuel sulfur by the International Maritime Organization allows us to test the sensitivity of the lightning to changes in ship plume aerosol number-size distributions. We find that, across a range of atmospheric thermodynamic conditions, the previously documented enhancement of lightning over the shipping lanes has fallen by over 40%. The enhancement is therefore at least partially aerosol-mediated, a conclusion that is supported by observations of droplet number at cloud base, which show a similar decline over the shipping lane. These results have fundamental implications for our understanding of aerosol-cloud interactions, suggesting that deep convective clouds are impacted by the aerosol number distribution in the remote marine environment.

Introduction

By acting as cloud condensation nuclei (CCN), aerosol particles influence clouds and, in turn, the Earth's energy balance. Aerosol-cloud interactions represent a significant uncertainty in our understanding of the Earth's climate (Boucher et al., 2013). Maritime ship traffic leads to the emission of aerosol particles and associated precursors into relatively clean marine air. These emissions enable study of how increased CCN perturb low-level marine stratus cloud droplet number distributions and related cloud macrophysical properties, such as cloud albedo and lifetime. (Diamond et al., 2020; Yuan et al., 2022; Durkee et al., 2000; Radke et al., 1989).

Deep convective cloud (DCC) systems occur throughout the tropics, and are essential to the Earth's water and energy cycles (Feng et al., 2021). However, there is little consensus on the mechanisms or magnitudes of aerosol particle impacts on DCCs (Tao et al., 2012; Seinfeld et al., 2016; Igel and van den Heever, 2021; Varble et al., 2023; ?). Thornton et al. (2017) documented a potential case of persistent maritime aerosol-DCC interactions analogous to stratocumulus ship tracks, with the discovery of enhancements in lightning over major shipping lanes passing through the Indian Ocean and South China Sea (Fig. 1).

Several mechanisms have been proposed to explain how aerosol particles from ship emissions could enhance lightning frequency, all of which involve enhanced cloud droplet nucleation (Twomey, 1977), leading to either 1) perturbations to super-cooled liquid water and ice hydrometeor distributions and enhanced charge separation in the mixed-phase region of DCC (Mansell and Ziegler, 2013; Blossey et al., 2018; Sun et al., 2024; Takahashi and Miyawaki, 2002; Deierling et al., 2008); or 2) an increase in the frequency or intensity of deep convection due to changes in the vertical distribution of humidity (Abbott and Cronin, 2021) or heating (Fan et al., 2018; Grabowski and Morrison, 2020). Some combination of 1 or 2 is also possible.

In January 2020, the International Maritime Organization (IMO) reduced the amount of allowable sulfur in fuel by a factor of seven, from 3.5% to 0.5% to curb effects of maritime shipping on air pollution (IMO, 2020). Recent analyses of shallow stratocumulus marine clouds over shipping lanes find changes to cloud brightness, droplet number, and droplet size associated with the IMO regulation, presumably due to the shift in aerosol number-size distribution (Watson-Parris et al., 2022; Yuan et al., 2022; Diamond, 2023).

We investigate whether the IMO fuel sulfur regulation has impacted lightning over the shipping lanes in the tropical Indian Ocean and South China Sea. We find the shipping lane lightning enhancement decreases significantly with the onset of the IMO regulation and that this decrease persists across a range of atmospheric conditions. We further show that the mean cloud droplet number concentration of shallow warm clouds over the Indian Ocean shipping lane was enhanced before the IMO regulation and also exhibits a decrease since the IMO regulation. We discuss the implications of these new results for mechanisms of shipping lane lightning enhancement and aerosol-DCC interactions.

Approach and findings

The Port of Singapore accounts for 20% of the world's bunkering fuel demand. The two primary shipping lanes it services—the Indian Ocean and South China Sea (hereafter "the shipping lanes")—have nearly an order of magnitude higher traffic than other shipping lanes around the world (Figure 1, top panel) (Mao et al., 2022). As shown in Figure 1 (middle panel), prior to 2020, the mean absolute lightning stroke density measured by the World Wide Lightning Detection Network (WWLLN) remains enhanced over these shipping lanes, consistent with Thornton et al. (2017). Since 2020, however, when the IMO regulation of sulfur emissions began, lightning over the shipping lanes has decreased to an annual stroke density about $1 \text{ stroke km}^{-2} \text{ year}^{-1}$ lower than before the regulation (Figure 1, bottom panel). While some of the largest absolute declines in lightning since 2020 occur over the shipping lanes, lightning has increased or decreased in other parts of this region as well. As we illustrate below, variability in the dynamic and thermodynamic context for convection over these shipping lanes must be taken into account to better isolate the potential impacts of shipping emissions.

Regional ship traffic, as measured by vessel fuel sales at the Port of Singapore, has been relatively constant or even increased since 2020 (Figure S1) (Port of Singapore, 2024). The disruption by COVID-19 did not obviously decrease activity at the port, seeming only to have briefly slowed the growth of cargo throughput for 2-3 months in 2020 (Gu et al., 2023). Therefore, we focus on controlling for the variability in background meteorological conditions that impact the frequency and intensity of convection, and thus lightning, over the shipping lanes.

We first examine the shipping lane lightning enhancement using two controls on background meteorology: 1) we only sample precipitating clouds (Huffman et al., 2015; Pradhan and Markonis, 2023; Watters et al., 2023); and 2) we restrict analyses to the specific seasons in each region favorable for lightning (November to April in the Indian Ocean; June to November in the South China Sea). Using these criteria, we composite lightning observations as a function of distance to the shipping lanes, the center of which we define as the peak in shipping emissions from the EDGAR emissions inventory (see Methods). As shown in Figure 2a, mean absolute lightning exhibits a clear enhancement over the shipping lane before 2020 (pre-IMO), between approximately 150km south to 150km north of the shipping lanes, and that has decreased since the regulation onset in 2020 (post-IMO) (Figure 2a).

To account for inter-annual variability in the frequency and intensity of convection in the region, we regress the observed annual lightning at a given distance from the shipping lane against three variables known to relate to lightning frequency (Convective Available Potential Energy (CAPE, discussed further below), precipitation rates (Romps et al., 2018), and the annual mean Oceanic Niño Index (ONI)) as well as several spatial variables such as latitude and longitude (Appendix A). Inter-annual variability in the MJO was small and had a negligible impact when included in the regression (see SI). The regressed variables explain 65% of variance of the annual means. We subtract the regressed lightning

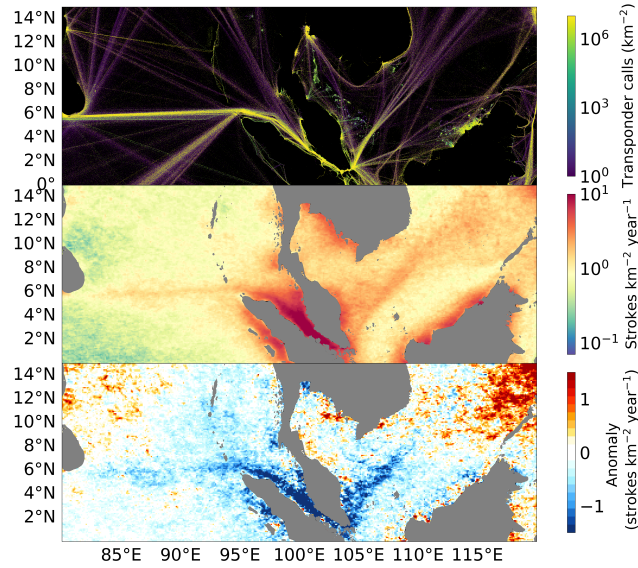


Fig. 1. (top) Map showing the total number of Automatic Identification Systems (AIS) transponder calls from 2015-2021, used by maritime vessels for collision avoidance. Data from the IMF World Seaborne Trade dataset (Cerdeiro et al., 2020). (middle) Climatological mean lightning stroke density near the Port of Singapore (2010-2019). (bottom) Difference of the post-regulation period (2020-2023) lighting stroke density from the 2010-2019 climatology above. See Appendix for further discussion of the retrievals.

from the observed annual mean, leaving the anomalous mean lightning stroke density that cannot be explained by interannual variability in storm occurrence and intensity, shown in Figure 2b.

The annual anomalous enhancement in lightning over the shipping lanes prior to 2020 is even clearer after regressing out meteorological variability, as is the near step-change decrease in the anomaly after 2020 (2b). Prior to the IMO regulation, essentially 100% of fuel sold at the port was high-sulfur (2b, right axis); correspondingly, the lightning anomaly over the shipping lane was $3.9 \text{ strokes km}^{-2} \text{ year}^{-1}$ on average and was never below $2.5 \text{ strokes km}^{-2} \text{ year}^{-1}$ for more than one year at a time. Adoption of the IMO regulation was prompt in 2020, as indicated by the change in high-sulfur fuel from 100% to less than 35% of fuel sold at the Port of Singapore. The Port of Singapore experienced little attenuation of fuel sales at the onset of COVID-19 (Gu et al., 2023), and total fuel sales have increased since 2020 consistent with higher traffic (Figure S1). Since 2020, the shipping lane lightning enhancements compared to adjacent regions have declined by 67% to $1.25 \text{ strokes km}^{-2} \text{ year}^{-1}$ on average.

To further control for higher-frequency variations in convective activity and intensity, we examine the lightning enhancement in a 2-dimensional CAPE and precipitation space, using 3-hourly coincident observations of CAPE, precipitation, and lightning. Cheng et al. (2021), building on Romps et al. (2018), showed that $\text{CAPE} \times \text{precipitation}$ is a reasonable proxy for tropical oceanic lightning frequency, given that a CAPE threshold is implemented. The 3-hourly CAPE and precipitation observations implicitly capture variability arising from more indirect sources, such as sea surface temperatures (SST), MJO events, fronts, etc (see SI for further discussion).

We compute lightning frequency in each CAPE-Precipitation bin using data from a region centered over each shipping lane and from reference regions adjacent to the shipping lanes (see Figure S2). We then compute a relative enhancement in lightning over the shipping lanes, before and after the onset of the IMO regulation, by taking the difference between corresponding CAPE-Precipitation bin-means in the shipping lane and associated reference box. The resulting shipping lane lightning enhancements as a function of both CAPE and Precipitation are shown in Figure 3. Before the IMO regulation (Pre-IMO), a shipping lane lightning enhancement existed in nearly every thermodynamic setting (e.g.,

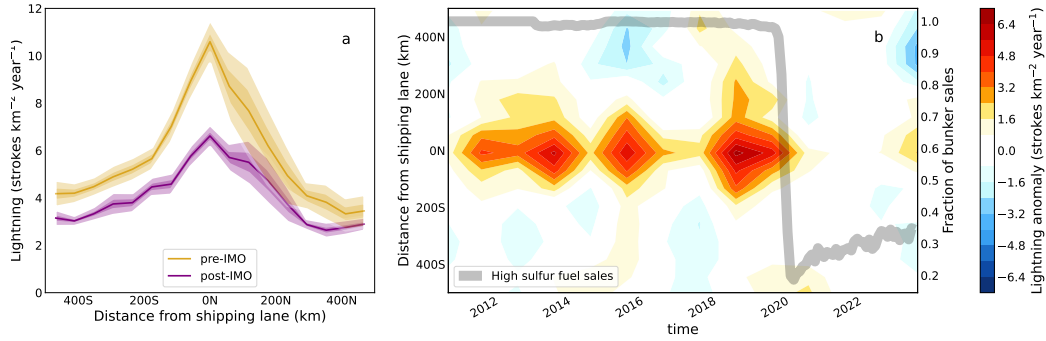


Fig. 2. (a) Lightning stroke density composited as a function of distance to the shipping lanes before and after the IMO regulation. Shading represents $\pm 2SE$ and $\pm 3SE$ (b) Hovmöller diagram of the annual mean lightning anomaly from the linear regression using Convective Available Potential Energy, precipitation, and Oceanic Niño Index from reanalysis data and observations, as well as spatial variables (latitude, longitude, $lat \cdot lon$, lat^2 , lon^2) (see text and SI for more details).

in each CAPE-Precipitation bin, Figure 3a,d) for both shipping lanes. As indicated by the larger pre-IMO perturbation, it seems that low-CAPE environments may have been more susceptible to aerosol enhancement of lightning.

Since the IMO regulation (Post-IMO), both shipping lanes exhibit significantly weaker lightning enhancements across most CAPE-Precipitation regimes (Figure 3b,e). The bin-by-bin differences between the Pre and Post-IMO lightning enhancement histograms are shown in Figure 3 (c and f). On average across all CAPE-Precip conditions, the lightning enhancement has decreased by 76% and by 47% for the Indian Ocean and South China Sea shipping lanes, respectively (Figure 3c,f). That is, for the same convective setting characterized by CAPE and Precipitation rates, the enhancement in lightning over the shipping lanes (as compared to adjacent regions) is significantly smaller after 2020 than it was before 2020.

Based upon the above, we hypothesize that the decline in the lightning enhancement since 2020 is most consistent with the IMO regulation changing CCN in the region. If decreasing sulfur emissions over the shipping lanes has reduced the total number of viable CCN and disrupted an associated mechanism for lightning enhancement, then there should be a corresponding change in warm cloud microphysics. To further test our hypothesis, we use Moderate Resolution Imaging Spectroradiometer (MODIS) satellite observations of cloud droplet number (N_d) in low clouds over the Indian Ocean shipping lane, where the influence of land is weaker and ship emissions are stronger, during the high-lightning season. The retrievals of N_d follow the method outlined in Zhu et al. (2018) (see Appendix A). Retrievals of N_d can only be done for shallow cumulus, not DCC. As a result, N_d retrievals sample a different set of conditions than the lightning observations. We assume that the behavior of N_d in shallow cumulus clouds from the same region is related to, though not necessarily a direct proxy for, N_d at cloud base in DCC.

In Figure 4, we show that prior to the IMO regulation, there is a clear trend in N_d toward land (north), as well as a clear perturbation in N_d over the shipping lane. This N_d perturbation is roughly 10-15% above the average of droplet concentrations 150km north and 150km south, which is larger than the shipping lane perturbations to N_d detected by Diamond et al. (2020) in Southeast Atlantic stratocumulus clouds. The N_d perturbation over the Indian Ocean shipping lane is a significant finding on its own, as observations of persistent, mean-state N_d perturbations by ships are rare (Diamond and Wood, 2020), especially for convectively active regions we show here.

Since the IMO regulation, the N_d away from the shipping lane mostly maintain their previous levels, as indicated by the overlap in the 95% confidence intervals, particularly to the north (upwind). Meanwhile, the enhancement in N_d over the shipping lane has become essentially undetectable. The decline in N_d over the shipping lane relative to the surrounding region establishes additional support for a relationship between the declining lightning enhancement and a shift in aerosol particle number-size distributions over the shipping lanes induced by the IMO regulation. N_d derived from shallow cumulus clouds will not be directly proportional to the CCN available for activation

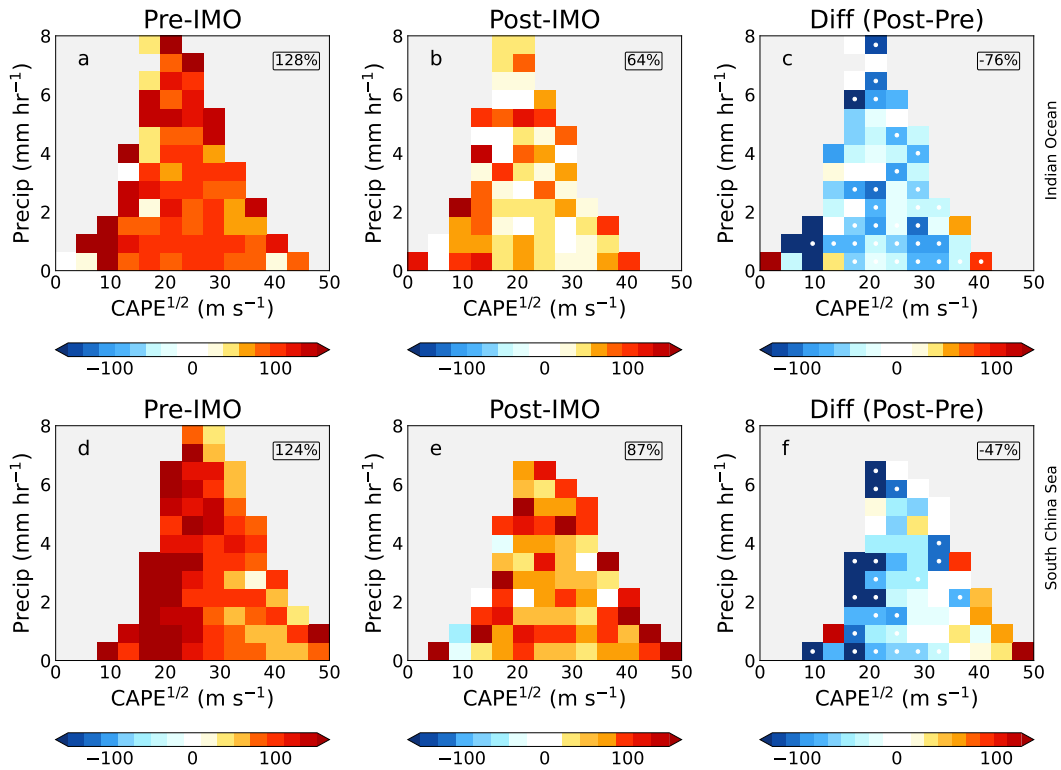


Fig. 3. Mean shipping lane percent enhancement in lightning stroke density (i.e., the relative difference in lightning over the shipping lane from that over immediately adjacent regions, see text), shown as colored pixels, binned by square root of CAPE reanalysis data (x-axis) and precipitation observations (y-axis) for the Indian Ocean (a)–(c) and South China Sea (d)–(f) shipping lanes. Enhancements since the regulation (b, e) are lower than before the regulation (a, d). The difference between post- and pre-IMO periods of the shipping lane lightning enhancements are represented in (c, f), where stippled bins indicate significance (p less than 0.05).

in high-supersaturation DCC (Hobbs et al., 2000), nor to the lightning enhancements that might result from CCN enhancements. However, the change in N_d is an additional observable indication, independent of the lightning observations, that the IMO regulations have clearly shifted aerosol particle distributions over the shipping lanes of interest here.

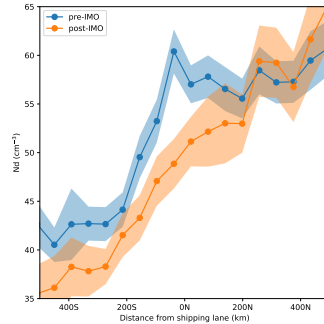


Fig. 4. Warm cloud-base droplet number (N_d) concentrations over the Indian Ocean, derived from MODIS observations of optical depth and effective radius following the procedure from Zhu et al. (2018). The pre-IMO regulation period is 2010-2019. Note the general increasing trend northward through the domain toward greater land influence, and the broad localized enhancement over the shipping lane prior to the regulation. To remove the effects and trends of large biomass burning and dust events, we remove any N_d retrievals where dust concentrations increase above $1 \mu\text{g m}^{-3}$ or black carbon concentrations above $0.1 \mu\text{g m}^{-3}$ (approximately the 50th percentile in each case). Shading represents $\pm 2\text{SE}$.

Implications

We find that a previously identified enhancement in lightning stroke density over the two major shipping routes near the Port of Singapore has declined by over 40% since 2020, when the IMO regulation of maritime shipping sulfur emissions came into effect. The decline is evident after controlling for natural variations in environmental conditions that characterize the convection intensity and frequency (see Figure 3). While ships may act as lightning attractors (Peterson, 2023), there is not evidence of a change in the number of ships traversing these shipping lanes over this time period (Figure S1). Further, an independently observed perturbation to N_d over the Indian Ocean shipping lane prior to the IMO regulation has since nearly vanished, indicating a coincident change in CCN over the region. The concomitant decline of N_d and lightning, timed with the onset of compliance with the IMO regulation, provides new evidence to support the set of CCN-mediated hypotheses previously proposed for invigoration of lightning (Fan et al., 2018; Abbott and Cronin, 2021; Mansell and Ziegler, 2013; Grabowski and Morrison, 2020).

Precisely how increases in CCN and N_d caused by ship emissions might lead to enhanced lightning remains unresolved. Both the pre-IMO and post-IMO perturbations to N_d are smaller than the enhancements of lightning, which may be explained by high scavenging rates in DCC during the high lightning season, as well as the different supersaturation conditions sampled by the N_d (shallow cumulus) and lightning retrievals (deep convection), non-linear relationships between N_d and ice secondary ice production, and ice nucleation.

Seppälä et al. (2021) find that a factor of 10 reduction in ship fuel sulfur content shifts emitted aerosol particles to smaller sizes and lower total number concentrations. Ultrafine particles $<50\text{nm}$ increase and those $>50\text{nm}$ decrease substantially, which implies that ultrafine particle invigoration of updraft velocities proposed in Fan et al. (2018) was not contributing to the shipping lane lightning enhancement pre-IMO. We conclude the lightning enhancement prior to the IMO regulation was mostly the result of higher concentrations of larger aerosol particles (e.g. $>50 \text{ nm}$) that perturbed: 1) cloud microphysics, such as elevated supercooled liquid water concentrations or rime splintering (see SI) (Mansell and Ziegler, 2013); and/or 2) updraft frequency, by means of heightened free tropospheric humidity or a mesoscale circulation response (Blossey et al., 2018; Grabowski and Morrison, 2020). Enhancements in ultrafine particles may play a role in the smaller non-zero shipping lane lightning enhancement that has persisted post-IMO.

The IMO regulation of ship fuel sulfur illustrates connections between international trade, air pollution, DCC microphysics, and lightning. Further work combining in situ and remote sensing of aerosol and cloud microphysics together with lightning frequency is needed to clarify the mechanisms behind these connections, and to quantify the relative roles of dynamic and microphysical responses. Our findings herein show that these regions remain a useful testbed for understanding aerosol pollution impacts on DCC and lightning.

Appendix A: Retrievals, data processing, and methods

Lightning stroke density observations come from the Worldwide Lightning Location Network (WWLLN), a ground-based lightning detection network with continuous global coverage of lightning at a resolution of 10km (Dowden et al., 2002). WWLLN uses very low frequency radio impulses (3-30 kHz) that, upon emission from a lightning stroke, propagates between the Earth-ionosphere waveguide and disperses into a wave train. The phase and frequency of that wave train determine the time of group arrival at three or more measurement stations, which can be used to back out the location of the stroke. While the detection efficiency for individual events is lower than satellite-based methods, continuous observations for more than a decade offer much more statistical power over our region of interest.

We use integrated multi-satellite retrievals for GPM (IMERG) precipitation rates (Huffman et al., 2015) and European Centre for Medium-Range Weather Forecasts (ECMWF) ReAnalysis-5th Generation (ERA5) atmospheric reanalyses (Hersbach et al., 2020) CAPE to compare the enhancement across various thermodynamic conditions. IMERG precipitation combines microwave and radar retrievals from TRMM and the GPM constellation. In ERA5, a value for CAPE is calculated for every departing level between the surface and 350hPa as follows:

$$CAPE = \int_{z_{dep}}^{z_{top}} g \left(\frac{\theta_{ep} - \bar{\theta}_{esat}}{\bar{\theta}_{esat}} \right) dz$$

where z_{dep} is the departing level, z_{top} is the level of neutral buoyancy, θ_{ep} is the virtual potential temperature of the parcel, and $\bar{\theta}_{esat}$ is the saturation virtual potential temperature of the environment. Once CAPE has been calculated for all levels, the most unstable layer is selected. We use $CAPE^{1/2}$, which is directly proportional to w_{max} , the theoretical maximum vertical velocity achievable at a location given the stability of the atmosphere. This follows from the proportionality between kinetic energy and the square of velocity. Further discussion of CAPE as it relates to lightning can be found in (Cheng et al., 2021) and (Romps et al., 2018).

Lightning in Figure 1 is shown on $0.1^\circ \times 0.1^\circ$ grid, calculated from 3-hourly lightning stroke densities. For subsequent calculations of the enhancement (Figures 2-3) all data (CAPE, precipitation, and lightning) is 3-hourly and mapped to a $0.5^\circ N \times 0.625^\circ E$ grid to minimize collocation errors and noise, and for comparison with MERRA-2 aerosol and meteorological reanalysis fields. Smoothly varying data (CAPE) is remapped bilinearly, while non-smoothly varying data (precipitation and lightning) are remapped conservatively (see Staff (2014) and sources therein for further detail on regridding practices). To provide some basic control for thermodynamic and meteorological variability, we only consider precipitating clouds (precipitation greater than 0.1mm/hr) during the high-lightning season (see SI).

We use data from 2010 onward, as WWLLN detection efficiency was still increasing rapidly prior to 2010. The shipping lanes are defined as regions where the Emissions Database for Global Atmospheric Research (EDGAR) $PM_{2.5}$ shipping emissions are greater than $5 \times 10^{-12} \text{ kg m}^{-2} \text{ s}^{-1}$ (Crippa et al., 2016). To remove influence from katabatic flows and sea-breeze driven convergence, we only consider the larger blue regions outlined in Figure S2. This notably removes the straight of Malacca, a region with both very high shipping emissions and active convection. There, surface convergence from land-based precipitation outflows on Sumatra and Malaysia and the adjacent landmasses make it challenging to establish a counterfactual, given the well-known land-ocean contrast in lightning stroke rates Cheng et al. (2021); Romps et al. (2018).

For Figure 2, the lightning stroke density (F) as a function of time (t) and distance from shipping lane (y) from the entire record is regressed as:

$$F(y, t) = \beta * X(y, t) + \epsilon$$

where X is the vector of predictors, (CAPE, precipitation, ONI, latitude (lat), longitude (lon), lat*lon, lat², lon²), β is the vector of coefficients. ϵ is the residual or "anomaly" that is shown in the figure. This anomaly represents the difference between the lightning one would expect given the environmental conditions ($\beta * X$) (see Figure S3) and the observed lightning (F). In accordance with Cheng et al. (2021) CAPE has been set to zero where CAPE^{1/2} \leq 15 ms⁻¹.

We utilized the "brightest 10%" method (Zhu et al., 2018; Cao et al., 2023) to obtain reliable N_d cloud droplet number concentration retrievals from MODIS Aqua across our target domain from 2010 to 2023. This method involves selecting the brightest 10% of clouds within each scene to calculate N_d values for every 0.5° x 0.5° grid box. The validity of this retrieval method has been corroborated through comparisons with ship-based observations (Efraim et al., 2020; Wang et al., 2021). N_d is computed using the cloud effective radius (r_e) and cloud optical depth (τ), as described by the equation:

$$N_d = \frac{\sqrt{5}}{2\pi k} \left(\frac{f_{ad} C_w \tau}{Q_{ext} \rho_w r_e^5} \right)^{\frac{1}{2}}$$

where k represents the volume radius ratio of cloud droplets (r_v) to r_e ($k = (r_v/r_e)^3 = 0.8$). The term f_{ad} denotes the adiabatic fraction, for which we assumed a constant value of 1 in our study, due to the absence of more refined alternatives (Bennartz and Rausch, 2017; Grosvenor et al., 2018). C_w signifies the adiabatic cloud water condensation rate within an ascending cloud parcel, expressed in grams per cubic meter per meter (g m⁻³ m⁻¹). The extinction efficiency factor, Q_{ext} , is assumed to be 2, and ρ_w is the density of water. To enhance the accuracy of our N_d estimations for each 0.5° x 0.5° grid box, we excluded pixels where the solar zenith angle exceeded 65 degrees (?). We also excluded of scenes containing mixed-phase, ice, or multilayer clouds. Consequently, after applying these filtering criteria, the remaining dataset comprised less than 1% of multilayer cloud pixels in any given grid. We use only the Indian Ocean shipping lane to maximize signal-to-noise, as the South China Sea has a much weaker signal due to its proximity to land and lower ship emissions. Inclusion of the South China Sea in the analysis does not alter the results. Finally, in order to remove the impact of dust storms advected over the Bay of Bengal, and to thereby reduce interannual variability in N_d outside the shipping lanes, we collocate 3-hourly MERRA-2 aerosol reanalysis output of dust and black carbon with the MODIS N_d retrievals. We then remove any N_d retrievals where dust concentrations increase above 1 ng m⁻³ or black carbon concentrations above 0.1 ng m⁻³ (approximately the 50th percentile in each case). Limited observations in the region likely hinder the ability of reanalysis products to capture the full variability in CCN sources (see SI for discussion of aerosol optical depth), possibly explaining some remaining differences in N_d over the southern region of the domain pre and post 2020.

Data availability

ERA5 CAPE may be downloaded using the Copernicus API at cds.climate.copernicus.eu. IMERG Precipitation and MERRA-2 aerosol are available for download at disc.gsfc.nasa.gov. ONI index is available at psl.noaa.gov/data/correlation/oni.data. Precipitation Feature reflectivity datasets are available for download at: <https://atmos.tamucc.edu/trmm/data/>. MODIS Aqua (MYD06) retrievals are available at ladsweb.modaps.eosdis.nasa.gov. Precipitation Feature reflectivity datasets are available for download at: <https://atmos.tamucc.edu/trmm/data/>. Global ship traffic density is available at: datacatalog.worldbank.org/search/dataset/0037580/Global-Shipping-Traffic-Density. Analysis and plotting available at 10.5281/zenodo.11373991 (Wright, 2024). WWLLN lightning location data are collected by a global scientific

collaboration and managed by the University of Washington. The WWLLN collaboration receives no federal, state or private funds to pay for the network operations, which are fully paid for by data sales (available at <https://wwlln.net>). Therefore, the stroke-level data is not free to the public. The composited annual stroke densities (as a function of distance from the shipping lane) and the mean pre- and post-regulation stroke densities region-wide are provided as part of the Zenodo code supplement.

Author Contributions

Analysis: CJW. Writing: CJW and JAT. Conceptualization and methodological development: CJW, JAT, LJ, and RW. N_d retrievals by: YC, YZ, JL. Additional expertise provided by RH, DR, RJ, PN, and DK

Acknowledgements

This work was funded by a grant from the U.S. National Science Foundation (AGS-2113494). Additional funding included (in order of authorship): Natural Science Foundation of China grant 42075093 (YC, YZ, JL), BSF Grant 2020809 (DR), NASA/UMBC grant NASA0144-01 (RW), NSF grant AGS-1912130 (PN), and New Faculty Startup Fund from Seoul National University (DK). The authors wish to thank the World Wide Lightning Location Network (<http://wwlln.net>), a collaboration among over 50 universities and institutions, for providing the lightning location data used in this paper.

Bibliography

- Abbott, T. H. and Cronin, T. W. (2021). Aerosol invigoration of atmospheric convection through increases in humidity. *Science*, 371(6524):83–85. Publisher: American Association for the Advancement of Science.
- Bennartz, R. and Rausch, J. (2017). Global and regional estimates of warm cloud droplet number concentration based on 13 years of AQUA-MODIS observations. *Atmospheric Chemistry and Physics*, 17(16):9815–9836. Publisher: Copernicus GmbH.
- Blossey, P. N., Bretherton, C. S., Thornton, J. A., and Virts, K. S. (2018). Locally Enhanced Aerosols Over a Shipping Lane Produce Convective Invigoration but Weak Overall Indirect Effects in Cloud-Resolving Simulations. *Geophysical Research Letters*, 45(17):9305–9313. .eprint: <https://onlinelibrary.wiley.com/doi/pdf/10.1029/2018GL078682>.
- Boucher, O., Randall, D., Artaxo, P., Bretherton, C., Feingold, G., Forster, P., Kerminen, V.-M., Kondo, Y., Liao, H., Lohmann, U., Rasch, P., Satheesh, S., Sherwood, S., Stevens, B., and Zhang, X. (2013). Clouds and Aerosols. pages 571–892.
- Cao, Y., Zhu, Y., Wang, M., Rosenfeld, D., Liang, Y., Liu, J., Liu, Z., and Bai, H. (2023). Emission Reductions Significantly Reduce the Hemispheric Contrast in Cloud Droplet Number Concentration in Recent Two Decades. *Journal of Geophysical Research: Atmospheres*, 128(2):e2022JD037417. .eprint: <https://onlinelibrary.wiley.com/doi/pdf/10.1029/2022JD037417>.
- Cerdeiro, Komaromi, Liu, and Saeed (2020). World Seaborne Trade in Real Time: A Proof of Concept for Building AIS-based Nowcasts from Scratch.
- Cheng, W.-Y., Kim, D., and Holzworth, R. H. (2021). CAPE Threshold for Lightning Over the Tropical Ocean. *Journal of Geophysical Research: Atmospheres*, 126(20):e2021JD035621. .eprint: <https://onlinelibrary.wiley.com/doi/pdf/10.1029/2021JD035621>.
- Crippa, M., Janssens-Maenhout, G., Dentener, F., Guizzardi, D., Sindelarova, K., Muntean, M., Van Dingenen, R., and Granier, C. (2016). Forty years of improvements in European air quality: regional policy-industry interactions with global impacts. *Atmospheric Chemistry and Physics*, 16(6):3825–3841. Publisher: Copernicus GmbH.
- Deierling, W., Petersen, W. A., Latham, J., Ellis, S., and Christian, H. J. (2008). The relationship between lightning activity and ice fluxes in thunderstorms. *Journal of Geophysical Research: Atmospheres*, 113(D15). .eprint: <https://onlinelibrary.wiley.com/doi/pdf/10.1029/2007JD009700>.
- Diamond, M. S. (2023). Detection of large-scale cloud microphysical changes within a major shipping corridor after implementation of the International Maritime Organization 2020 fuel sulfur regulations. *Atmospheric Chemistry and Physics*, 23(14):8259–8269. Publisher: Copernicus GmbH.
- Diamond, M. S., Director, H. M., Eastman, R., Possner, A., and Wood, R. (2020). Substantial Cloud Brightening From Shipping in Subtropical Low Clouds. *AGU Advances*, 1(1):e2019AV000111. .eprint: <https://onlinelibrary.wiley.com/doi/pdf/10.1029/2019AV000111>.
- Diamond, M. S. and Wood, R. (2020). Limited Regional Aerosol and Cloud Microphysical Changes Despite Unprecedented Decline in Nitrogen Oxide Pollution During the February 2020 COVID-19 Shutdown in China. *Geophysical Research Letters*, 47(17):e2020GL088913. .eprint: <https://onlinelibrary.wiley.com/doi/pdf/10.1029/2020GL088913>.
- Downen, R. L., Brundell, J. B., and Rodger, C. J. (2002). VLF lightning location by time of group arrival (TOGA) at multiple sites. *Journal of Atmospheric and Solar-Terrestrial Physics*, 64(7):817–830.
- Durkee, P. A., Noone, K. J., Ferek, R. J., Johnson, D. W., Taylor, J. P., Garrett, T. J., Hobbs, P. V., Hudson, J. G., Bretherton, C. S., Innis, G., Frick, G. M., Hoppel, W. A., O'Dowd, C. D., Russell, L. M., Gasparovic, R., Nielsen, K. E., Tessmer, S. A., Öström, E., Osborne, S. R., Flagan, R. C., Seinfeld, J. H., and Rand, H. (2000). The Impact of Ship-Produced Aerosols on the Microstructure and Albedo of Warm Marine Stratocumulus Clouds: A Test of MAST Hypotheses 1i and 1ii. *Journal of the Atmospheric Sciences*, 57(16):2554–2569. Publisher: American Meteorological Society Section: Journal of the Atmospheric Sciences.

- Efraim, A., Rosenfeld, D., Schmale, J., and Zhu, Y. (2020). Satellite Retrieval of Cloud Condensation Nuclei Concentrations in Marine Stratocumulus by Using Clouds as CCN Chambers. *Journal of Geophysical Research: Atmospheres*, 125(16):e2020JD032409. .eprint: <https://onlinelibrary.wiley.com/doi/pdf/10.1029/2020JD032409>.
- Fan, J., Rosenfeld, D., Zhang, Y., Giangrande, S. E., Li, Z., Machado, L. A. T., Martin, S. T., Yang, Y., Wang, J., Artaxo, P., Barbosa, H. M. J., Braga, R. C., Comstock, J. M., Feng, Z., Gao, W., Gomes, H. B., Mei, F., Pöhler, C., Pöhler, M. L., Pöschl, U., and de Souza, R. A. F. (2018). Substantial convection and precipitation enhancements by ultrafine aerosol particles. *Science*, 359(6374):411–418. Publisher: American Association for the Advancement of Science.
- Feng, Z., Leung, L. R., Liu, N., Wang, J., Houze Jr, R. A., Li, J., Hardin, J. C., Chen, D., and Guo, J. (2021). A Global High-Resolution Mesoscale Convective System Database Using Satellite-Derived Cloud Tops, Surface Precipitation, and Tracking. *Journal of Geophysical Research: Atmospheres*, 126(8):e2020JD034202. .eprint: <https://onlinelibrary.wiley.com/doi/pdf/10.1029/2020JD034202>.
- Grabowski, W. W. and Morrison, H. (2020). Do Ultrafine Cloud Condensation Nuclei Invigorate Deep Convection? Section: Journal of the Atmospheric Sciences.
- Grosvenor, D. P., Sourdeval, O., Zuidema, P., Ackerman, A., Alexandrov, M. D., Bennartz, R., Boers, R., Cairns, B., Chiu, J. C., Christensen, M., Deneke, H., Diamond, M., Feingold, G., Fridlind, A., Hünerbein, A., Knist, C., Kollias, P., Marshak, A., McCoy, D., Merk, D., Painemal, D., Rausch, J., Rosenfeld, D., Russchenberg, H., Seifert, P., Sinclair, K., Stier, P., van Dierenhoven, B., Wendisch, M., Werner, F., Wood, R., Zhang, Z., and Quaas, J. (2018). Remote Sensing of Droplet Number Concentration in Warm Clouds: A Review of the Current State of Knowledge and Perspectives. *Reviews of Geophysics*, 56(2):409–453. .eprint: <https://onlinelibrary.wiley.com/doi/pdf/10.1029/2017RG000593>.
- Gu, Y., Chen, Y., Wang, X., and Chen, Z. (2023). Impact of COVID-19 epidemic on port operations: Evidence from Asian ports. *Case Studies on Transport Policy*, 12:101014.
- Hersbach, H., Bell, B., Berrisford, P., Hirahara, S., Horányi, A., Muñoz-Sabater, J., Nicolas, J., Peubey, C., Radu, R., Schepers, D., Simmons, A., Soci, C., Abdalla, S., Abellan, X., Balsamo, G., Bechtold, P., Biavati, G., Bidlot, J., Bonavita, M., De Chiara, G., Dahlgren, P., Dee, D., Diamantakis, M., Dragani, R., Flemming, J., Forbes, R., Fuentes, M., Geer, A., Haimberger, L., Healy, S., Hogan, R. J., Hólm, E., Janisková, M., Keeley, S., Laloyaux, P., Lopez, P., Lupu, C., Radnoti, G., de Rosnay, P., Rozum, I., Vamborg, F., Villaume, S., and Thépaut, J.-N. (2020). The ERA5 global reanalysis. *Quarterly Journal of the Royal Meteorological Society*, 146(730):1999–2049. .eprint: <https://onlinelibrary.wiley.com/doi/pdf/10.1002/qj.3803>.
- Hobbs, P. V., Garrett, T. J., Ferek, R. J., Strader, S. R., Hegg, D. A., Frick, G. M., Hoppel, W. A., Gasparovic, R. F., Russell, L. M., Johnson, D. W., O'Dowd, C., Durkee, P. A., Nielsen, K. E., and Innis, G. (2000). Emissions from Ships with respect to Their Effects on Clouds. Section: Journal of the Atmospheric Sciences.
- Huffman, G. J., Bolvin, D. T., Braithwaite, D., Hsu, K., Joyce, R., Xie, P., and Yoo, S.-H. (2015). NASA global precipitation measurement (GPM) integrated multi-satellite retrievals for GPM (IMERG). *Algorithm theoretical basis document (ATBD) version*, 4(26):30. Publisher: NASA Goddard Space Flight Center Greenbelt, MD.
- Igel, A. L. and van den Heever, S. C. (2021). Invigoration or Enervation of Convective Clouds by Aerosols? *Geophysical Research Letters*, 48(16):e2021GL093804. .eprint: <https://onlinelibrary.wiley.com/doi/pdf/10.1029/2021GL093804>.
- IMO (2020). IMO 2020 Cutting Sulphur Oxide Emissions.
- Mansell, E. R. and Ziegler, C. L. (2013). Aerosol Effects on Simulated Storm Electrification and Precipitation in a Two-Moment Bulk Microphysics Model. *Journal of the Atmospheric Sciences*, 70(7):2032–2050. Publisher: American Meteorological Society Section: Journal of the Atmospheric Sciences.
- Mao, X., Rutherford, D., Osipova, L., and Georgeff, E. (2022). Exporting emissions: Marine fuel sales at the Port of Singapore. Technical report.
- Peterson, M. (2023). Interactions Between Lightning and Ship Traffic. *Earth and Space Science*, 10(11):e2023EA002926. .eprint: <https://onlinelibrary.wiley.com/doi/pdf/10.1029/2023EA002926>.
- Port of Singapore (2024). Bunkering Statistics.
- Pradhan, R. K. and Markonis, Y. (2023). Performance Evaluation of GPM IMERG Precipitation Products over the Tropical Oceans Using Buoys. *Journal of Hydrometeorology*, 24(10):1755–1770. Publisher: American Meteorological Society Section: Journal of Hydrometeorology.
- Radke, L. F., Coakley, J. A., and King, M. D. (1989). Direct and Remote Sensing Observations of the Effects of Ships on Clouds. *Science*, 246(4934):1146–1149. Publisher: American Association for the Advancement of Science.
- Romps, D. M., Charn, A. B., Holzworth, R. H., Lawrence, W. E., Molinari, J., and Vollaro, D. (2018). CAPE Times P Explains Lightning Over Land But Not the Land-Ocean Contrast. *Geophysical Research Letters*, 45(22):12,623–12,630. .eprint: <https://onlinelibrary.wiley.com/doi/pdf/10.1029/2018GL080267>.
- Seinfeld, J. H., Bretherton, C., Carslaw, K. S., Coe, H., DeMott, P. J., Dunlea, E. J., Feingold, G., Ghan, S., Guenther, A. B., Kahn, R., Kraucunas, I., Kreidenweis, S. M., Molina, M. J., Nenes, A., Penner, J. E., Prather, K. A., Ramanathan, V., Ramaswamy, V., Rasch, P. J., Ravishankara, A. R., Rosenfeld, D., Stephens, G., and Wood, R. (2016). Improving our fundamental understanding of the role of aerosol-cloud interactions in the climate system. *Proceedings of the National Academy of Sciences*, 113(21):5781–5790. Publisher: Proceedings of the National Academy of Sciences.
- Seppälä, S. D., Kuula, J., Hyvärinen, A.-P., Saarikoski, S., Rönkkö, T., Keskinen, J., Jalkanen, J.-P., and Timonen, H. (2021). Effects of marine fuel sulfur restrictions on particle number concentrations and size distributions in ship plumes in the Baltic Sea. *Atmospheric Chemistry and Physics*, 21(4):3215–3234. Publisher: Copernicus GmbH.
- Staff, N. (2014). The Climate Data Guide: Regridding Overview.
- Sun, R., Lu, X., Gao, M., Du, Y., Lin, H., Wright, C., He, C., and Yin, K. (2024). The impacts of shipping emissions on lightning: roles of aerosol-radiation-interactions and aerosol-cloud-interactions. *Environmental Research Letters*, 19(3):034038. Publisher: IOP Publishing.
- Takahashi, T. and Miyawaki, K. (2002). Reexamination of Riming Electrification in a Wind Tunnel. *Journal of the Atmospheric Sciences*, 59(5):1018–1025. Publisher: American Meteorological Society Section: Journal of the Atmospheric Sciences.
- Tao, W.-K., Chen, J.-P., Li, Z., Wang, C., and Zhang, C. (2012). Impact of aerosols on convective clouds and precipitation. *Reviews of Geophysics*, 50(2). .eprint: <https://onlinelibrary.wiley.com/doi/pdf/10.1029/2011RG000369>.
- Thornton, J. A., Virts, K. S., Holzworth, R. H., and Mitchell, T. P. (2017). Lightning enhancement over major oceanic shipping lanes. *Geophysical Research Letters*, 44(17):9102–9111. .eprint: <https://onlinelibrary.wiley.com/doi/pdf/10.1002/2017GL074982>.
- Twomey, S. (1977). The Influence of Pollution on the Shortwave Albedo of Clouds. *Journal of the Atmospheric Sciences*, 34(7):1149–1152. Publisher: American Meteorological Society Section: Journal of the Atmospheric Sciences.

- Varble, A. C., Igel, A. L., Morrison, H., Grabowski, W. W., and Lebo, Z. J. (2023). Opinion: A critical evaluation of the evidence for aerosol invigoration of deep convection. *Atmospheric Chemistry and Physics*, 23(21):13791–13808. Publisher: Copernicus GmbH.
- Wang, Y., Zhu, Y., Wang, M., Rosenfeld, D., Gao, Y., Yao, X., Sheng, L., Efraim, A., and Wang, J. (2021). Validation of satellite-retrieved CCN based on a cruise campaign over the polluted Northwestern Pacific ocean. *Atmospheric Research*, 260:105722.
- Watson-Parris, D., Christensen, M. W., Laurenson, A., Clewley, D., Gryspeerdt, E., and Stier, P. (2022). Shipping regulations lead to large reduction in cloud perturbations. *Proceedings of the National Academy of Sciences*, 119(41):e2206885119. Publisher: Proceedings of the National Academy of Sciences.
- Watters, D. C., Gattlin, P. N., Bolvin, D. T., Huffman, G. J., Joyce, R., Kirstetter, P., Nelkin, E. J., Ringerud, S., Tan, J., Wang, J., and Wolff, D. (2023). Oceanic Validation of IMERG-GMI Version 6 Precipitation Using the GPM Validation Network. *Journal of Hydrometeorology*, 25(1):125–142. Publisher: American Meteorological Society Section: Journal of Hydrometeorology.
- Wright, C. (2024). Lightning Declines Over Shipping Lanes Follow Regulation of Fuel Sulfur: Data Analysis.
- Yuan, T., Song, H., Wood, R., Wang, C., Oreopoulos, L., Platnick, S. E., von Hippel, S., Meyer, K., Light, S., and Wilcox, E. (2022). Global reduction in ship-tracks from sulfur regulations for shipping fuel. *Science Advances*, 8(29):eabn7988. Publisher: American Association for the Advancement of Science.
- Zhu, Y., Rosenfeld, D., and Li, Z. (2018). Under What Conditions Can We Trust Retrieved Cloud Drop Concentrations in Broken Marine Stratocumulus? *Journal of Geophysical Research: Atmospheres*, 123(16):8754–8767. .eprint: <https://onlinelibrary.wiley.com/doi/pdf/10.1029/2017JD028083>.

Supplemental Information

Ship traffic

As noted in the main manuscript, fuel sales statistics from the Port of Singapore are a reasonable proxy for the amount of large ship activity in the two shipping lanes considered here. While not accounting for vessels that might fuel elsewhere prior to transiting one of the shipping lanes, it is likely that if a ship transits the Indian Ocean shipping lane to Singapore it will fuel there for a subsequent journey through the South China Sea (or a return to the Indian Ocean) and vice versa for a ship first transiting the South China Sea. Thus, that gross fuel sales for large vessels at the Port of Singapore has remained largely constant or even increased since 2020 (see Figure S1) suggests fairly minimal changes in ship traffic through these two shipping lanes. There is nothing like a 50% drop in shipping that might explain the change in lightning.

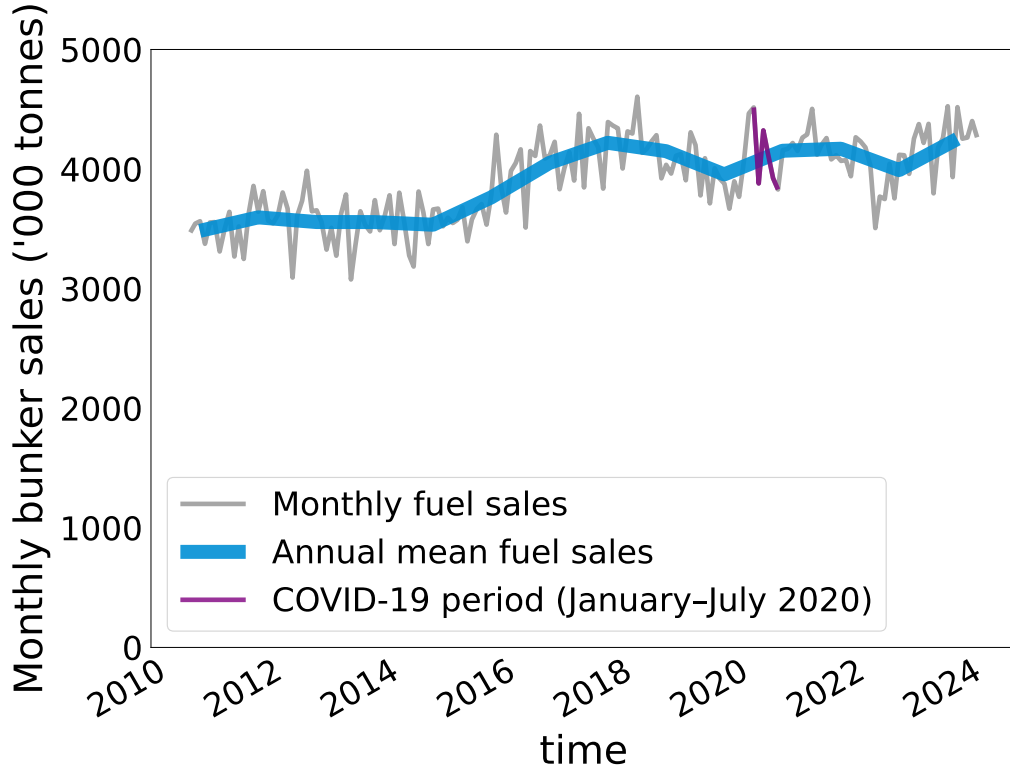


Fig. S1. Total fuel sales at the Port of Singapore have been generally increasing

Our approach to lightning stroke density analysis differs slightly from that of Thornton et al., (2017), in that only the Southern Indian Ocean reference region is used for CAPE–Precip analysis due to its similarity to the Indian Ocean shipping lane in frequency of convection and precipitation during the high-lightning season (November to April). Conducting the same analysis with the Northern Indian Ocean reference region does not alter the conclusions of this analysis. Blue boxes in Figure S2 show regions used for compositing lightning and N_d as a function of distance from the shipping lane.

Over both shipping lane regions, seasonal to subseasonal variability is dominated by the migration of the ITCZ, also called the monsoon, as well as the Madden-Julian Oscillation (MJO). The high lightning season in each region occurs when the ITCZ migrates over the shipping lane before reaching a stable location a few hundred kilometers away. This passage of the ITCZ, on top of periodic MJO-related convection, cause considerable variability in the background within a single high lightning season and across years. For this reason, we analyze the data first on

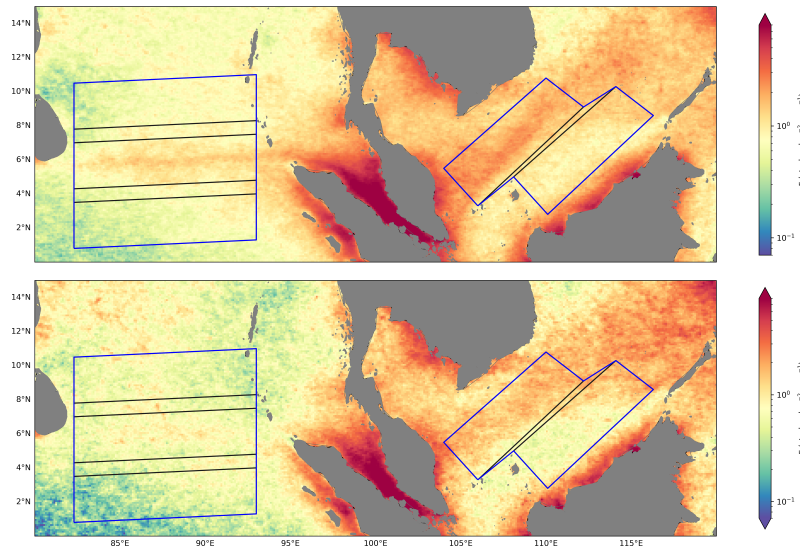


Fig. S2. Climatology (top) as in Figure 1, but with the boxes indicated in black that are used for calculating the shipping lane lightning enhancements as a function of CAPE and Precipitation presented in Figure 3. Stroke density since the regulation (bottom) used to make the difference plot in Figure 2.

an annual basis, taking an entire high lightning (monsoon) season (Figure 2 in the main manuscript), to complement the more rigorous high resolution (3-hourly) analysis shown in Figure 3 in the main manuscript.

For calculating the anomalous lightning enhancement over the shipping lanes shown in Figure 2B of the main manuscript, we regress out of the lightning stroke density the interannual variations in CAPE, Precipitation, and large scale climate variability represented by the ENSO ONI index. The predicted lightning stroke density using these variables outside of the shipping lane is shown in Figure S3 below.

In both Figure 2B and Figure 3 in the main manuscript, we remove the effects of CAPE and precipitation, which are considered reliable measures of MJO and monsoon activity and intensity (Zhang et al., 2022). To illustrate the predictive value of CAPE and precipitation in the region, we provide an example of a non-normalized CAPE–Precip diagram for the Indian Ocean pre–IMO S4. These analyses also control for interannual variability of ITCZ strength as well as variations in MJO phase. Moreover, the intraseasonal variability associated with the MJO, shown in S5, has no clear trend since 2020 and thus its specific role in the changes in the lightning enhancement is negligible.

SST-driven fluxes on heat and moisture may also be important for setting the stage for convection to occur and for driving instability; however, the connection between SSTs and lightning is less obvious than that for the more direct measures of instability (CAPE and precipitation) used here. For a more in-depth analysis of the SST-pattern drivers of convection and ITCZ migration in this region, we refer the reader to Zhang et al. (2022).

Reflectivity

Thornton et al (2017) showed that DCC over the shipping lane exhibited anomalously higher radar reflectivity in the mixed phase region prior to 2015, but we find statistically robust tests of changes in DCC reflectivity since the IMO regulation are not yet possible. We use the GPM precipitation feature database from Chuntao Liu’s group to probe the shipping lane enhancement of cold, strong reflectivity echoes (Liu et al., 2008). Note that this approach to examining reflectively is slightly different from that done in Thornton et al. (2017), but follows that in Blossey et al. (2018). Due to infrequent sampling and small swath width, the reflectivity signal shown here requires very long records to show the effect of the shipping lane (previous studies, such as Blossey et al. (2018), use the full TRMM record, which is well over a decade). Splitting

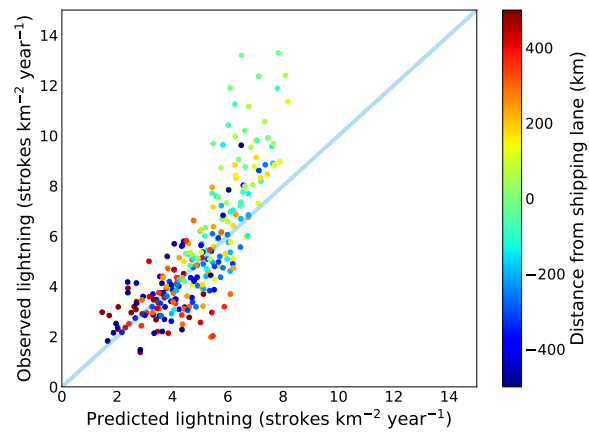


Fig. S3. Observed vs predicted lightning stroke density in the vicinity of the shipping lanes. Annual mean predictions are from linear regression of lightning stroke density against CAPE, precipitation, ONI, latitude (lat), longitude (lon), lat*lon, lat², and lon². Colors show the distance from the shipping lane. R² is 0.65.

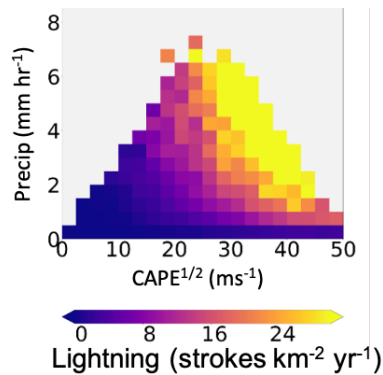


Fig. S4. Mean stroke density near the Indian Ocean shipping lane, binned by CAPE and precipitation, as in Figure 3 of the main text.

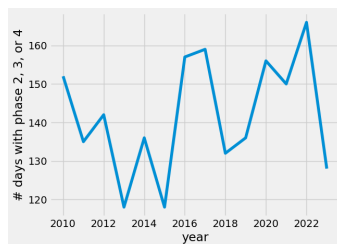


Fig. S5. Number of days with MJO phase 2, 3, or 4 from Realtime Multivariate MJO Index (RMM). This indicator of intraseasonal variability shows no clear trend since 2020

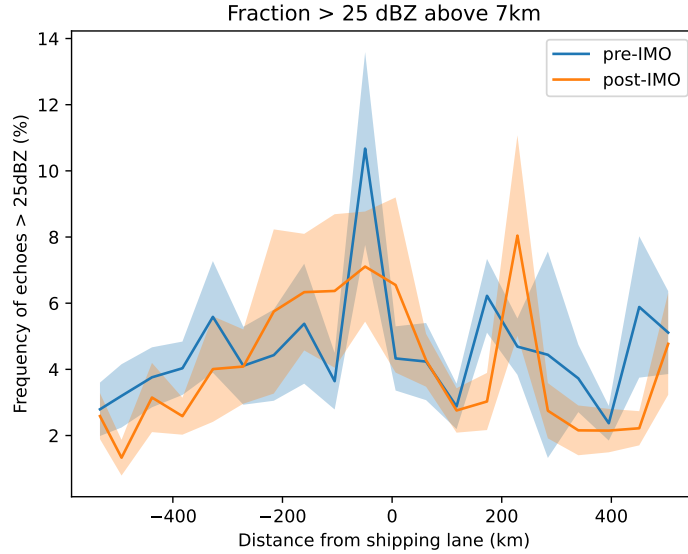


Fig. S6. Frequency of cold echoes (25dBZ or greater, above 8km) from GPM, discussed in Blossey et al (2018) and citations therein as a proxy for lightning. The peak in reflectivity has diminished since the regulation, but weak sampling power does not allow us to confirm this change (the pre-IMO record is restricted GPM’s record, i.e. years since 2016).

the relatively short (8 year) GPM record of reflectivity into a pre- and post-IMO period therefore greatly reduces the statistical power of the retrievals. Indeed, the peak in reflectivity established over the shipping lane between 2016 and 2019 has diminished (Figure S5). However, the difference between the two periods is not statistically significant (p less than 0.05), and we therefore refrain from concluding that there has or has not been a change to reflectivity above the shipping lanes.

Why not use AOD?

As noted in the main manuscript, we expect that perturbations to CCN in the shipping lane regions is best represented by MODIS N_d retrievals, rather than by AOD because 1) clear sky conditions are rare in this region leading to limited AOD retrievals and consequently limited statistical power and 2) AOD being proportional to aerosol cross sectional area columns does not directly correspond to CCN number at cloud base, the subject of this paper. For example, as shown in Figure S6, AOD estimates from MERRA-2 reanalysis, nudged by both their aerosol model and the limited AOD observations by MODIS, exhibit no observable enhancement over the shipping lanes prior to or after the 2020 IMO regulation. This lack of AOD enhancement is expected given that ship emissions of aerosol particles are concentrated in smaller, less radiatively active particle sizes [see, e.g., Hobbs et al. (2000) and Seppälä et al. (2021)], statistical sampling is limited by infrequent cloud-free scenes, and that particle scavenging and dilution rates in these regions are relatively high due frequent convection.

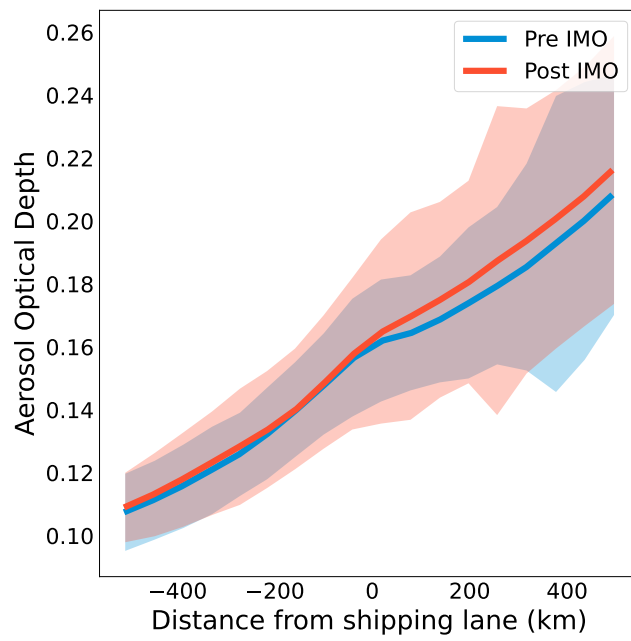


Fig. S7. Mean Aerosol Optical Depth from MERRA-2 as a function of distance from the shipping lane. Shading indicates 95% confidence.

Bibliography

- Blossey, P. N., Bretherton, C. S., Thornton, J. A., and Virts, K. S. (2018). Locally Enhanced Aerosols Over a Shipping Lane Produce Convective Invigoration but Weak Overall Indirect Effects in Cloud-Resolving Simulations. *Geophysical Research Letters*, 45(17):9305–9313. .eprint: <https://onlinelibrary.wiley.com/doi/pdf/10.1029/2018GL078682>.
- Hobbs, P. V., Garrett, T. J., Ferek, R. J., Strader, S. R., Hegg, D. A., Frick, G. M., Hoppel, W. A., Gasparovic, R. F., Russell, L. M., Johnson, D. W., O'Dowd, C., Durkee, P. A., Nielsen, K. E., and Innis, G. (2000). Emissions from Ships with respect to Their Effects on Clouds. Section: *Journal of the Atmospheric Sciences*.
- Liu, C., Zipser, E. J., Cecil, D. J., Nesbitt, S. W., and Sherwood, S. (2008). A Cloud and Precipitation Feature Database from Nine Years of TRMM Observations. Section: *Journal of Applied Meteorology and Climatology*.
- Seppälä, S. D., Kuula, J., Hyvärinen, A.-P., Saarikoski, S., Rönkkö, T., Keskinen, J., Jalkanen, J.-P., and Timonen, H. (2021). Effects of marine fuel sulfur restrictions on particle number concentrations and size distributions in ship plumes in the Baltic Sea. *Atmospheric Chemistry and Physics*, 21(4):3215–3234. Publisher: Copernicus GmbH.
- Thornton, J. A., Virts, K. S., Holzworth, R. H., and Mitchell, T. P. (2017). Lightning enhancement over major oceanic shipping lanes. *Geophysical Research Letters*, 44(17):9102–9111. .eprint: <https://onlinelibrary.wiley.com/doi/pdf/10.1002/2017GL074982>.
- Zhang, H., Seager, R., and Xie, S.-P. (2022). How Does Sea Surface Temperature Drive the Intertropical Convergence Zone in the Southern Indian Ocean? *Journal of Climate*, 35(16):5415–5432. Publisher: American Meteorological Society Section: *Journal of Climate*.